Dynamics of Swelling/Contracting Hard Spheres Surmised by an Irreversible Langevin Equation†

Alexander V. Popov,‡ Justin Melvin, and Rigoberto Hernandez*

Center for Computational and Molecular Science and Technology, School of Chemistry and Biochemistry, Georgia Institute of Technology, Atlanta, Georgia 30332-0400

Received: August 1, 2005; In Final Form: October 28, 2005

The diffusion of molecules through uniform homogeneous materials can readily be described by Brownian motion or generalizations thereof. The further generalization of these models to describe molecular diffusion through heterogeneous and nonstationary solvents is much less understood. Phenomenological nonstationary generalizations of the generalized Langevin equation (GLE) have earlier been developed satisfying the fluctuation−dissipation relationship in quasi-equilibrium limits while exhibiting somewhat complex behavior away from equilibrium. This reduced-dimensional representation should be capable of describing the diffusion of a particle through a colloidal suspension whose average particle size is tuned by an external driving force such as pH. A simple particle model of such a process involves the motion of a hard-sphere particle in an explicit environment of swelling hard spheres. The velocity autocorrelation functions observed in a large number of simulations of the particle model under various swelling rates agree precisely with those of a single form of the nonstationary phenomenological model. Though this procedure is not an explicit projection of the mechanical system onto the nonstationary GLE, it does show that the latter correctly describes the dynamics of the projected coordinate—namely, diffusion of the solute—under nonequilibrium conditions. Both nonequilibrium solvent models lead to behavior reminiscent of β-relaxation processes at packing fractions substantially below that of the glass transition.

I. Introduction

A typical approach for simplifying the complex dynamics in chemical and biophysical processes involves the identification of a one- (or reduced-) dimensional reaction path or order parameter characteristic of the dynamical event. Unfortunately, such simplifications are often not possible because the projection of the solvent onto the usual stochastic models presumes that the solvent response is linear. Reduced-dimensional models can nonetheless be used to qualitatively capture the nonequilibrium dynamics exhibited by complex systems, albeit by including nonlocal and nonstationary terms. Though such reduced-dimensional models are often phenomenological in construction, our group has shown that such a formalism can approximately arise from the projection of a nonconservative Hamiltonian involving a uniform time-dependent coupling to a harmonic bath.[1,2] A more provocative argument in favor of such representations, however, would lie in the construction of a particle model whose projected dynamics may be surmised by it. Indeed, this work explicitly constructs the nonstationary memory kernel for a nonequilibrium hard-sphere model by numerical simulation under various sets of nonequilibrium conditions and finds precise agreement with the phenomenological model in which the dynamics is dissipated by an implicit nonstationary solvent.

An explicit phenomenological model describing nonstationary processes has been constructed by extending the generalized Langevin equation (GLE) to include multiplicative noise that can be controlled in space, in time, and self-consistently to the dynamics itself.[3,4] This model has been called the irreversible generalized Langevin equation (iGLE) in deference to the additional irreversibility that arises due to the multiplicative noise. Although the theoretical and computational analysis of this class of equations has shown qualitative agreement with a number of experimental systems,[5−8] to date there have been neither direct experimental nor molecular simulation results confirming the appropriateness of the iGLE. Nevertheless, in ref 2, the iGLE has been shown to agree with the numerical simulations of a chosen coordinate that is uniformly coupled to all the bath coordinates through the single multiplicative factor, $g(t)$. The latter is also the term that carries the multiplicative noise in the iGLE. The Ohmic (or memory-less) limit of the iGLE would be a Langevin equation with multiplicative noise. This so-called iLE will be seen here to suffice in describing the dynamics of the model system.

The coupling term in the iLE tunes the interactions between the chosen coordinates and the solvent response uniformly. A real model in which such a mechanism should be operative would presumably involve a tagged solute solvated by a uniformly changing solvent. This is precisely what appears to be happening when one follows the dynamics of a particular colloid moving through a colloidal suspension which either swells or shrinks in time. Several groups[9−15] are presently investigating the structural and dynamical properties of solutions of colloidal and microgel particles which are able to change their size due to the high response to temperature and pH alterations. Under such conditions, the particle diameters can swell by as much as an order of magnitude in a couple of milliseconds.[14,16,17] This dynamical process is modeled in this article as that of a Brownian particle driven by a nonequilibrium environment. The model provides insight on the observed

† Part of the special issue "William Hase Festschrift".

* To whom correspondence should be addressed. E-mail: hernandez@chemistry.gatech.edu.

‡ Permanent address: Technological Institute, Kemerovo 650056, Russia.

10.1021/jp054241a CCC: $33.50
Published on Web 12/18/2005

processes while also providing insight on nonstationary (nonequilibrium) dynamics, in general.

The outline of this article is as follows: In part II, a simple particle model is described in order to capture the dynamics of a hard-sphere particle diffusing through a solvent of hard spheres whose radii are time dependent, for example, swelling. The numerical considerations for integrating the equation of motion are also discussed therein. The projective nonstationary equations of motion, the iGLE and the iLE, are reviewed in section III in preparation for the connection to be drawn between them and the nonstationary particle model. (The projection of the time-dependent Hamiltonian to the iGLE is described in the Appendix.) In ref 1, the iGLE was derived under the assumption that the coupling terms with bath modes are proportional to one and the same function, $g(t)$. But, in real systems, a nonuniform interaction should be expected when the coupling to the ith bath mode is characterized by a specific $g_i(t)$. In section III, we also show that, in the Ohmic limit, the iLE arises regardless of the distribution of $g_i(t)$, when the effective coupling term, $g(t)$, is taken in some sense as an average of all the $g_i(t)$ terms. Numerical analysis of the simulations is presented in part IV. The fact that the velocity autocorrelation function of the chosen particle in a nonequilibrium environment can be surmised by the iLE is the central result of this article.

II. Nonstationary Diffusion in a Swelling-Particle Solvent

The model system consists of a heavy hard-sphere particle immersed within a solvent of lighter hard-sphere particles. It differs from Brownian motion because of the presence of nonequilibrium (time-dependent) solvation by way of the swelling or contracting of the lighter particles as specified a priori. The structural change affects the effective volume fraction and consequently the motion of the chosen Brownian particle. Such is the only nonstationary condition imposed upon the solvent particles and through them, on the chosen particle. This generic model system could, for example, describe the diffusion of a colloidal particle in a colloidal suspension in which the latter is subject to shape changes through the pH-induced addition or depletion of water.

The specific parameters used in the simulations reported below include the masses, $m = 4 \times 10^{-16}$ g and $M = 2 \times 10^{-14}$ g, of the light and heavy particles, respectively. The entire system of 300 light particles and one heavy particle is placed into a cubic reservoir with sides set to $L = 2800$ nm. The imposition of periodic boundary conditions on this system relies on the fact that the heavy particle finds itself in the infinitely dilute limit. To ensure that the results are converged with respect to overall system size, several measures have been compared to those for a system with 600 solvent particles in a box with twice the volume. Though not shown here for lack of space, there is no significant difference between the VACFs of the Brownian particle in either box dimension, for example. This confirms both the convergence with system size and the assumed dilute-solute condition.

The shape changes in the solvent particles are specified by way of their radii r. For simplicity, the latter are taken as a linear function in time, that is

$$r = r_0 + wt \tag{2.1}$$

where r_0 is the initial radius (typically chosen to equal 30 nm), and w is the swelling rate (taken to be 0, 0.5, ± 1, 2, and ± 3 nm/ms in section IV). The maximal simulation time was chosen to be $t_{max} = 100$ ms for $w < 2$ nm/ms, 80 ms for $w = 2$ nm/ms, and 60 ms for $w = 3$ nm/ms. The maximal radius of swelling particles at $w = 3$ nm/ms is $r_m = 210$ nm. At this endpoint, the volume fraction of solvent particles becomes 0.53. The radius $R = 100$ nm of the colloidal particle does not change.

The well-known hard-sphere algorithm was used to integrate the dynamics of the system.[18] It is easy to code and has been verified using various standard convergence checks. The hard-sphere algorithm greatly improves the performance of the integration because the variable time step is maximized so as to evolve the particles ballistically between collisions in a single step. The time-dependent changes in the solvent particles, however, complicate the algorithm in at least two ways. The first is that the time to collision must be altered to account for the increased width of the solvent particles. In the linear growth case, this can still be predicted analytically and the algorithm was modified accordingly. The second results from the fact that a swelling particle could in principle induce a mechanical force on a colliding particle. This force, however, is ignored, and the energy of a colliding pair of particles is preserved before and after a collision. This constraint allows the system to maintain constant energy (as specified through an effective temperature, $T = 300$ K) without introducing additional constraints.

An additional difficulty in numerically integrating this system arises when the relative velocity of two particles after a collision becomes smaller than $2w$. In such cases, the growth of these special particles is stopped in order to prevent them from overlapping until such time when new collisions kick them apart. Thereafter, the special particles are once again swelled at the original rate. Note that all other particles continue to swell throughout this time. Though seemingly bothersome, we found that, at the chosen swelling rates, the number of such instances is so small that the deviation of the average value of particle radius r from that predicted by eq 2.1 never exceeded 0.1%.

III. Nonstationary Diffusion in a Projective Model

A. Irreversible Langevin Equation (iLE). A particle may experience an inhomogeneous viscous drag as it diffuses through a system. When this drag is effectively reproducible as a function of the coordinates, the diffusion of such particles has been described using stochastic models which are dissipated by a space-dependent multiplicative noise.[19−23] The equation of motion can be written in the form

$$\dot{v}(t) = -\int_0^t g(x(t))\gamma_{th}(t-t')g(x(t'))v(t')\,dt' + g(x(t))\xi_{th}(t) \tag{3.1}$$

where (x,v) are the explicit (possibly multidimensional) position and velocity variables associated with the reduced-dimensional space describing the particle, namely, the chosen coordinates. Here, $\gamma_{th}(t)$ is the friction kernel representing the uniform delayed response of the solvent in the space-independent case, and $\xi_{th}(t)$ is the random force obeying the fluctuation−dissipation theorem

$$\langle \xi_{th}(t)\xi_{th}(t')\rangle = k_B T\,\gamma_{th}(t-t') \tag{3.2}$$

Equation 3.1 differs from the usual generalized Langevin equation (GLE) because of the presence of the coupling term, $g(x(t))$. This term modulates the noise amplitude and reflects the inhomogeneity of the space-dependent friction. Equation 3.1 has been derived as the projection of harmonic bath modes coupled nonlinearly to the chosen coordinate.[19−23] Much work has been dedicated to theoretical investigation of this equation and its numerical calculation.[24−26]

The coupling of the chosen coordinates to the bath can change with time if the environment undergoes a temporal alteration. This can lead to an additional time-dependent response which contributes to the friction. In the case that there is no spatial dependence in the random force, the stochastic equation—namely, the irreversible GLE (iGLE)—reads[1,3]

$$\dot{v}(t) = -\int_0^t g(t)\gamma_{th}(t-t')g(t')v(t')\,dt' + g(t)\xi_{th}(t) \quad (3.3)$$

where $g(t)$ is completely determined by an irreversible process that is indirectly driving the system. Equation 3.3 has a multiplicative form similar to (3.1), but the inhomogeneity in the nonstationarity is in time rather than in space. In fact, the approach developed in refs 2, 4, and 5 includes the more general cases in which the multiplicative term, g, can arise from inhomogeneities in time, in space, and as a result of self-consistent coupling with other tagged particles. In the special case of time-dependent friction most relevant to this work, the dynamics of the chosen coordinates propagated by the iGLE has been seen to obey the fluctuation−dissipation relation (FDR).

The Ohmic or local limit of the GLE arises when the memory kernel decays infinitely fast, reducing to

$$\gamma_{th}(t) = 2\gamma_0\delta(t) \quad (3.4)$$

The dynamics of the corresponding Langevin equation (LE) is well-known to be accurate for the description of the motion of a heavy particle in liquid.[27] In this limit, the iGLE (3.3) turns into the simpler form

$$\dot{v}(t) = -g^2(t)\gamma_0 v(t) + g(t)\xi_0(t) \quad (3.5)$$

$$\langle \xi_0(t)\xi_0(t')\rangle = 2k_B T\gamma_0\delta(t-t')$$

which will be called the "irreversible Langevin equation" (iLE). Note that the integration in eq 3.3 keeps only "half" of the δ-function, so that $2\gamma_0$ reduces to γ_0 in eq 3.5. The iLE has been used earlier by Hershkovits and Hernandez to describe the dynamics of a rotating mesogen in a liquid crystal.[8]

B. Equivalent Mechanical System. The microscopic origin of the nonstationarity in the iGLE (and iLE) can be illustrated through a simple infinite-dimensional mechanical system that was earlier shown to project onto a collective coordinate driven by the iGLE.[1,2] Following ref 1, but generalizing the spectral coefficients c_i to depend on time nonuniformly by way of the ith coupling term $g_i(t)$, the nonstationary Hamiltonian can be written as

$$H = \frac{p_q^2}{2} + \frac{1}{2}\sum (p_i^2 + \omega_i^2 x_i^2) - \sum c_i g_i(t) x_i q + \delta V_1(q,t) + \delta V_2(q(\cdot),t) \quad (3.6)$$

where

$$\delta V_1(q,t) = \frac{1}{2}\sum \left(\frac{c_i g_i(t)}{\omega_i}\right)^2 q^2 \quad (3.7)$$

is the renormalization of the potential which eliminates the spectral shift. The correction δV_2 to the memory can be determined according to eqs 2.7c−2.8 of ref 1, namely

$$\delta V_2(q(\cdot),t) = \frac{1}{2}\int_0^t dt'\, a(t,t')[q(t') - q(t)]^2 - \frac{1}{2}q(t)^2\int_0^1 dt'\, a(t,t') \quad (3.8)$$

where

$$a(t,t') \equiv \sum g_i(t)\dot{g}_i(t')\frac{c_i^2}{\omega_i^2}\cos\omega_i(t-t')$$

and each of the coupling terms $g_i(t)$ are now allowed to depend on the ith mode. Without loss of generality, the initial condition for the latter can be chosen as

$$g_i(0) = 1 \quad (3.9)$$

which is equivalent to specifying the early-time thermal friction by way of the initial time-independent coupling constants, c_i.

The form of the nonstationary Hamiltonian in eq 3.6 is perhaps disturbing in that the δV_2 term contains nonlocal terms that refer to some special initial time (called 0 therein) and therefore are arbitrary for general forms of $g(t)$. This problem is partially resolved, however, by ensuring that this reference time was in the distant past when the system was in equilibrium. During this domain of times, $\dot{g}(t')$ is zero and, consequently, so is $a(t,t')$ and the contributions to δV_2. Nevertheless, the presence of the nonstationary terms necessarily introduces troubling questions about time-reversal symmetry and the causality principle. The former issue is precisely the reason the investigation of the projective model is of interest, and the connection to the swelling-sphere model discussed in the next section helps to shed light on it. The latter issue manifests itself most clearly in the construction of the projected equation of motion described in the Appendix.

Subject to the assumptions detailed above and in the Appendix, the equation of motion for the chosen coordinate q is

$$\ddot{q} = -\int_0^t \gamma(t,t')\dot{q}(t')\,dt' + \xi(t) \quad (3.10)$$

where

$$\gamma(t,t') = \sum \frac{c_i^2}{\omega_i^2} g_i(t)\cos\omega_i(t-t')g_i(t') \quad (3.11)$$

$$\xi(t) = \sum \frac{c_i}{\omega_i} g_i(t)\left(p_i(0)\sin\omega_i t + \left(\omega_i x_i(0) - \frac{c_i}{\omega_i}q(0)\right)\cos\omega_i t\right) \quad (3.12)$$

with the usual FDR

$$\langle \xi(t)\xi(t')\rangle = \frac{1}{\beta}\gamma(t,t') \quad (3.13)$$

If all the functions $g_i(t)$ are equal to $g(t)$, then the right-hand side (RHS) of eq 3.11 can be simplified to

$$\gamma(t,t') = g(t)g(t')\gamma_{th}(t-t') \quad (3.14)$$

with

$$\gamma_{th}(t-t') = \sum \frac{c_i^2}{\omega_i^2}\cos\omega_i(t-t') \quad (3.15)$$

representing the friction in the static case as well as the early-time initial condition described above. Thus, the iGLE in eq 3.3 is recovered as obtained earlier in ref 1.

The transition to the pure Markovian (memory-less) cases eqs 3.4 and 3.5 can be made by an appropriate choice of the friction kernel. Following the usual procedure,[28−30] eq 3.15 can be rewritten for the continuous spectrum as

$$\gamma_{\text{th}}(t-t') = \frac{2}{\pi}\int_0^\infty \cos\omega(t-t')\frac{J(\omega)}{\omega}\,\mathrm{d}\omega \qquad (3.16)$$

where $J(\omega)$ is the spectral density. A typical choice of the latter, which is also made here, is

$$J(\omega) = \gamma_0\frac{\omega}{1+\omega^2\tau^2} \qquad (3.17)$$

with τ being the characteristic "memory" time. After calculating the integral in eq 3.16, one obtains the usual form of an exponential decay in the memory friction

$$\gamma_{\text{th}}(t-t') = 2\gamma_0\frac{\exp(-|t-t'|/\tau)}{2\tau} \qquad (3.18)$$

The $\tau \to 0$ limit of this expression results in the iLE of eqs 3.4 and 3.5.

The same strategy can be applied to show that even in the more general case of nonuniform coupling (see eq 3.11), the iLE is still retrieved. Introducing the continuous function $\tilde{g}(t,\omega)$ to replace the discrete coefficients $g_i(t)$ into the friction kernel of eq 3.11 leads to the result

$$\gamma(t,t') = \frac{2}{\pi}\int_0^\infty \tilde{g}(t,\omega)\tilde{g}(t',\omega)\cos\omega(t-t')\frac{J(\omega)}{\omega}\,\mathrm{d}\omega \qquad (3.19)$$

Assuming that $\tilde{g}(t,\omega) = \tilde{g}(t,-\omega)$, the lower limit in the integral can be extended down to $-\infty$. With the additional insertion of eq 3.17, the friction kernel further transforms to the integral

$$\gamma(t,t') = \frac{\gamma_0}{\pi}\int_{-\infty}^\infty \tilde{g}(t,\omega)\tilde{g}(t',\omega)\frac{\cos\omega(t-t')}{1+\omega^2\tau^2}\,\mathrm{d}\omega \qquad (3.20)$$

$$= \frac{\gamma_0}{\pi}\int_{-\infty}^\infty \tilde{g}(t,\omega)\tilde{g}(t',\omega)\cos\omega(t-t')\frac{i}{2\tau}\left[\frac{1}{\omega+i\tau^{-1}} - \frac{1}{\omega-i\tau^{-1}}\right]\mathrm{d}\omega$$

By noting the poles in the integrand as well as their limiting values at large $|\omega|$ values, these integrals can readily be evaluated in the complex plane in terms of their residues

$$\gamma(t,t') = 2\gamma_0\frac{\exp(-|t-t'|/\tau)}{2\tau}\,\mathscr{R}[\tilde{g}(t,i\tau^{-1})\,\tilde{g}(t',i\tau^{-1})] \qquad (3.21)$$

Only those values of t and t' that differ on the order of τ contribute to the memory kernel. In the limit that τ is small, the memory kernel, eq 3.21, effectively depends only on t, namely, it is approximately local in time. However, even in this limit, the memory kernel remains nonstationary as it contains a t-dependent term not present in eq 3.18.

The nonstationarity in the memory kernel can be simplified by approximating eq 3.21 as

$$\gamma(t,t') \approx 2\gamma_0\frac{\exp(-|t-t'|/\tau)}{2\tau}\,G^2(t^*,\tau) \qquad (3.22)$$

where

$$G^2(t^*,\tau) \equiv \mathscr{R}[\tilde{g}^2(t^*,i\tau^{-1})] \qquad (3.23)$$

and t^* is some arbitrary time between t and t'. (A judicious choice of t^* could make this exact once again but that would reintroduce the complexity we are trying to avoid.) In the memory-less $\tau \to 0$ limit of the iLE, for example, eq 3.22 reduces to

$$\gamma(t,t')|_{\tau=0} = 2\gamma_0\delta(t-t')G^2(t^*,\tau)|_{\tau=0} \qquad (3.24)$$

where t^* likewise is simply equal to t. For $\tau \neq 0$, a connection between the term $G^2(t^*,\tau)$ and the coupling constants can be obtained using the $t = t' = t^*$ limit after equating eqs 3.11 and 3.21

$$\gamma(t^*,t^*) = \sum\frac{c_i^2}{\omega_i^2}g_i^2(t^*) = \frac{\gamma_0}{\tau}\,\mathscr{R}[\tilde{g}^2(t^*,i\tau^{-1})] \equiv \frac{\gamma_0}{\tau}\,G^2(t^*,\tau) \qquad (3.25)$$

At early times, the discrete initial condition ($g_i(t) \equiv 1$ for all i) can be cast into a continuous form for which $\tilde{g}(t,\omega) = 1$. This leads to the simple connection

$$\sum\frac{c_i^2}{\omega_i^2} = \frac{\gamma_0}{\tau} \qquad (3.26)$$

between the discrete coupling coefficients and the integrated friction and time constant. The term in eq 3.23 is thus the weighted value of all the $g_i^2(t^*)$ terms

$$G^2(t^*,\tau) = \frac{\sum g_i^2(t^*)c_i^2/\omega_i^2}{\sum c_i^2/\omega_i^2} \qquad (3.27)$$

(This equation is valid for all τ which, although not seen in the RHS, is defined through the coupling coefficients implicitly.) Comparison with the iGLE in the uniform coupling case and noting eq 3.24 suggest that the weighted value of all $g_i^2(t)$ can act as a single uniform coupling term, $G^2(t)$, in the iLE.

It is useful to note that the LE is recovered in the limit of a nonswelling solvent. That is, if the swelling is stopped at time t_{stop}, the coupling functions $g_i(t) \equiv \tilde{g}(t,\omega_i)$ become constant at $t > t_{\text{stop}}$. It is reasonable to suppose that they have no peculiarities at $\omega \to \infty$ and that there exists a limiting value $g_{\text{stop}} \equiv \tilde{g}(t_{\text{stop}},\omega \to \infty)$, which is a real number. Inserting this limiting value in eqs 3.23, 3.24, and then in eq 3.5, one immediately recovers the usual LE.

IV. Results and Discussion

Simulations of the particle model described in section II under both swelling ($w > 0$) and contracting ($w < 0$) conditions have been performed. In all cases, the velocity autocorrelation function (VACF) for the Brownian particle has been generated. The VACFs appear to follow a single universal function upon reduction of the variables using a form suggested by the solution of the VACF for a corresponding iLE model. Inversion of this single universal function, by way of the iLE solution from section III, yields an exact expression for the time-dependent coupling term $g(t)$. It scales with the collision frequency ν of the Brownian particle which, in its turn, is directly connected to geometrical properties of the system (radii of the particles and their volume fraction). This universal scalability also

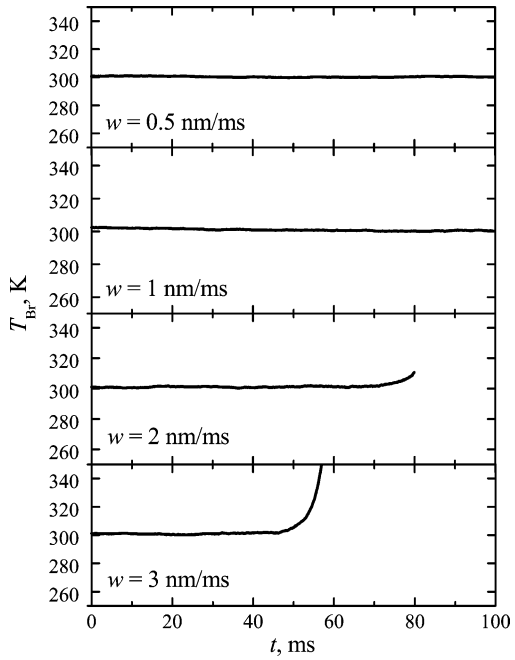

Figure 1. Kinetic energy of the Brownian particle expressed through temperature units at various w values.

suggests an interdependence between the kinetic parameters (VACFs, diffusion coefficient D) and structural properties.

A. Scaling VACF for Swelling Solvent Particles. In Figure 1, the kinetic energy of the Brownian particle is presented in temperature units, $T_{Br} = E_K/(^3/_2 k_B)$. With few exceptions, it is approximately equal to the temperature, 300 K, of the solvent when the swelling rate is small. At the faster swelling rates, $w = 2-3$ nm/ms, T_{Br} rises dramatically toward the end of the simulation. Therein, the packing volume fraction of the solvent spheres reaches values above that of the freezing transition (0.494) when arrested behavior commences.[31,32] At the faster swelling rates, the glassy solvent particles are trapped in nonequilibrium solvation structures and hence do not necessarily respond linearly to the Brownian particle nor dissipate it appropriately. That is, the quasi-equilibrium condition breaks down. The concerted phenomenon presumably involves a response function that contains memory and hence its behavior cannot be captured by the iLE.

The VACFs

$$C_w(t_0,t) \equiv \frac{\langle v(t_0)v(t)\rangle}{\langle v^2(t_0)\rangle} \tag{4.1}$$

for various swelling rates w and initial times t_0 are shown in Figure 2. If indeed the VACFs for this system can be described by the iLE discussed above, then they should behave like

$$C_w(t_0,t) = \exp[-\gamma_0 \int_{t_0}^{t} g_w^2(t')\, dt'], \quad t_0 < t \tag{4.2}$$

which is the solution of eq 3.5 for the VACF in terms of the unknown coupling term $g_w(t)$. The smooth curves overlaying the numerical VACFs in Figure 2 are precisely the fits of eq 4.2, and they are generally in good agreement. At a fast swelling rate, $w = 3$ nm/ms, when $t - t_0$ is small (it is ca. 20 ms), the VACFs displayed in Figure 3 exhibit deviating oscillations with a small amplitude on the order of 0.001. These deviations are not unexpected as they occur in the same region in which quasi-

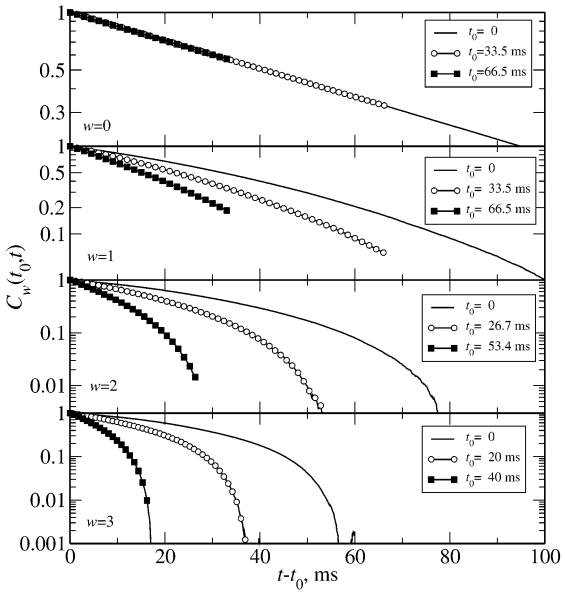

Figure 2. Time dependencies of the function $C_w(t_0,t)$ of the Brownian particle for three different delay times t_0 at various w values (shown in nm/ms).

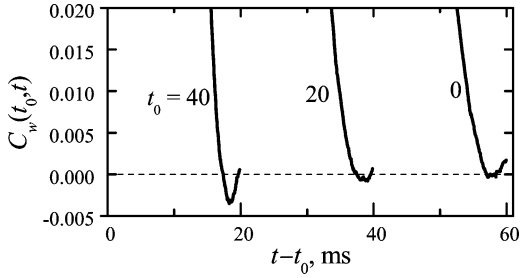

Figure 3. Negative dips in the VACFs for $w = 3$ nm/ms. The time t_0 is shown in ms.

equilibrium was seen to break down in Figure 1, and consequently, neither the iLE nor its solution, eq 4.2, are applicable therein.

The success in fitting eq 4.2 to the numerical VACFs further suggests that a more direct solution can be found if only $g_w(t)$ could be determined. At equilibrium, it is proportional to the collision frequency ν in accordance with Enskog theory[33] (at least, at small volume fractions), and one may expect that

$$\frac{g_w^2(t)}{g_w^2(0)} = \frac{\gamma_0 g_w^2(t)}{\gamma_0 g_w^2(0)} \approx \frac{\nu(t)}{\nu(0)} \tag{4.3}$$

Figure 4A displays ν as a function of t for various w in a semilog plot; the apparent linearity in the regime when the iLE was seen above to be applicable suggests that log ν can indeed be taken as a linear function in time. Moreover, for fast spatial equilibration (i.e., in the quasi-equilibrium regime), ν is a function only of the radius r because r defines the volume fraction which fully describes the thermodynamic state for the hard-sphere fluid. Thus at quasi-equilibrium, the frequency ν depends on w and t only through the product wt, which in turn determines the radius unambiguously. Hence, $g_w(t)$ can be written in terms of a universal function

$$g_w(t) = g_+(wt) \tag{4.4}$$

that depends only on the product, wt. In the simulations presented here, the swelling rates w are about an order of

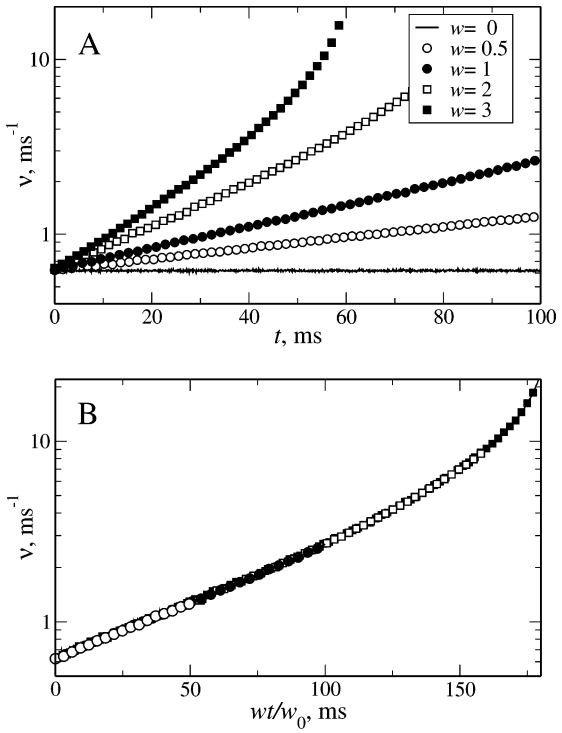

Figure 4. (A) Time dependence of the collision frequency between the Brownian and solvent particles at different w values (in units of nm/ms). (B) The same curves are rescaled horizontally: the temporal coordinate is extended by the factor of w/w_0 for each line (see explanation in the text).

magnitude smaller than the thermal velocity. Consequently, the system is always in quasi-equilibrium or close to it. Thus, g_+ nearly reflects the instantaneous coupling to the solvent at a given time t. These claims are validated further by Figure 4B, where all curves taken from Figure 4A are superposed after stretching the abscissa by a factor of w/w_0, where the reference w_0 was chosen to equal 1 nm/ms (for $w = 0.5$ nm/ms, the temporal coordinate is squeezed twice; for $w = 0$, the corresponding line reduces into point). The fact that the universality of the curve in Figure 4B appears to go beyond linearity suggests that eq 4.4 may hold well beyond the quasi-equilibrium limit in which it was obtained.

The iLE-based correlation function of eq 4.2, together with the conjectured connection of eq 4.4, leads to

$$\ln C_{w_0}(t_0,t) = -\gamma_0 \int_{t_0}^{t} g_+^{\,2}(w_0 t')\, \mathrm{d}t' \qquad (4.5)$$

$$= -\frac{w}{w_0}\gamma_0 \int_{w_0 t_0/w}^{w_0 t/w} g_+^{\,2}(ws)\, \mathrm{d}s$$

$$= \frac{w}{w_0} \ln C_w\left(\frac{w_0}{w} t_0, \frac{w_0}{w} t\right) \qquad (4.6)$$

where w_0 is the reference swelling rate, as above. In other words, if $C_w(t_0,t)$ is known for $w = w_0$, then any other VACF can be obtained through the transformation

$$\ln C_w(t_0,t) = \frac{w_0}{w} \ln C_{w_0}\left(\frac{w}{w_0} t_0, \frac{w}{w_0} t\right) \qquad (4.7)$$

This apparent law of corresponding states for the VACF with respect to the swelling rate is illustrated in Figure 5, where the VACFs, $C_w(0,t)$, from Figure 2 are scaled by the factor w/w_0 and shown as a function of wt/w_0. All the lines coincide, and

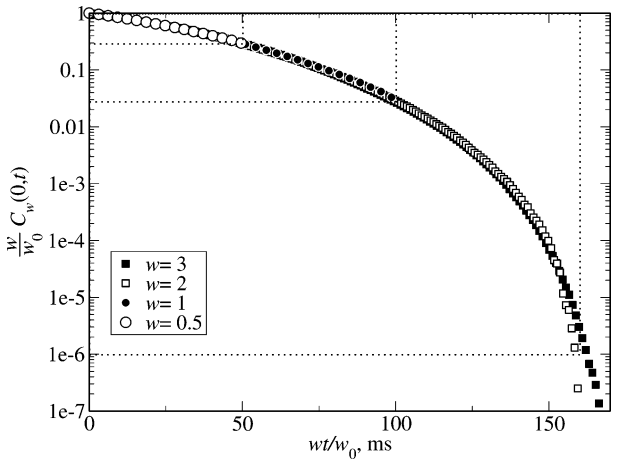

Figure 5. VACF, $C_w(0,t)$, taken from Figure 2, for various w values (in nm/ms), rescaled both vertically and horizontally in accordance with eq 4.7 (see explanation in the text).

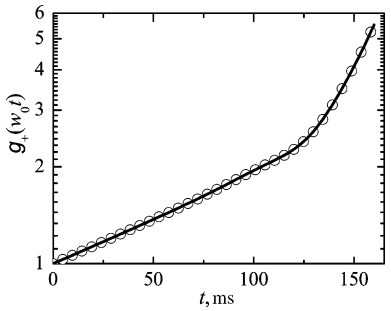

Figure 6. Coupling term $g_+(w_0t)$ at $w_0 = 1$ nm/ms as a function of time.

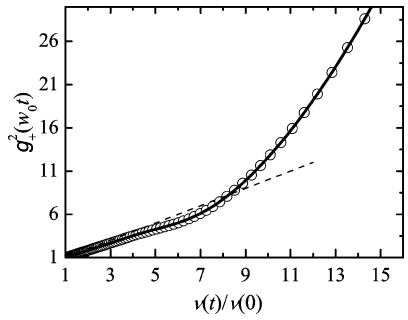

Figure 7. Coupling term $g_+(w_0t)$ at $w_0 = 1$ nm/ms as a function of the collision frequency ν. The dashed line represents relation 4.3.

the resulting line approaches zero at $t \approx 175$ ms where the volume fraction η is near 0.5 and is just below the glass transition.

The universal coupling function $g_+(wt)$ can be extracted from the simulations through a fit of the VACFs to eq 4.5. The error of this fit is smaller than the thickness of the fitted curve. The time dependence of log $g_+(w_0t)$ is shown in Figure 6. At early times, the curve is clearly linear suggesting initial quasi-Markovian behavior but then there is a dramatic increase above 140 ms. Meanwhile, $g_+^{\,2}(w_0t)$ is plotted vs the normalized collision frequency in Figure 7. Again, at early times there is apparent linearity—in fact, equality—before the deviation at later times. Nevertheless, eq 4.3 clearly holds at early times when the quasi-equilibrium condition is satisfied. But even when it does not strictly hold, it once again appears that the correspondence in eq 4.6 is universal.

B. Scaling VACF for Contracting Solvent Particles. Although the results of the previous section are encouraging, one might critique the fact that all of the cases started and ended

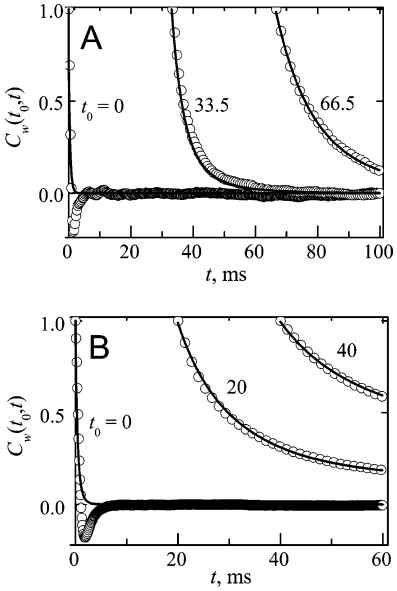

Figure 8. VACF, $C_w(t_0, t)$, at $w = -1$ nm/ms (A) and $w = -3$ nm/ms (B). The circles and curves present the simulation results and the iLE-based eq 4.2, respectively. The initial time t_0 is shown in ms.

at the same limits while the only change was an increase in the swelling rate. To test this, the model was simulated in the reverse direction: The simulations are begun with an equilibrated solvent consisting of bath particles with a large radius (= 210 nm) and is subsequently contracted linearly to a small radius (= 30 nm) at a specified rate. As these are contracting, the swelling rate is now negative. Two different cases, $w = -1$ and -3 nm/ms, are discussed here explicitly because they are representative of all of the observed behavior. If, indeed, the coupling function depends only on the instantaneous configuration of the solvent, and because the initial conditions have merely been reflected across the time interval, then it would be expected that the VACFs would still be described by the reference VACF as before. Note, however, that the time argument of the VACFs must now be adjusted to $(t_{max} - t)$ where t_{max} is the total time over which the solvent particles swell (or contract). The universal coupling function $g_-(\cdot)$ in the contracting case can be written in terms of $g_+(\cdot)$ as

$$g_-(wt) = g_+(w(t_{max} - t))$$

The numerical VACFs are shown in Figure 8 and agree with the iLE-based correlation functions remarkably well. The only exception to this agreement appears at early times when simulation data exhibits a negative dip for the VACF at $t_0 = 0$. It is significantly more pronounced than that observed in Figure 3 above. This fact can be easily understood if we recall that at the initial conditions for the contracting solvent system, the solvent is dense with a packing fraction near 0.53. As it is equilibrated before the simulations begin, this solvent is sufficiently dense so as to cage the Brownian particle (and itself) leading to correlated collisions.[34,35] Such correlations give rise to memory in the solvent response, but they are clearly not present in the local friction used in the iLE. Hence, the contracting solvent (when not too dense) exhibits iLE behavior and is characterized by the same universal function that was seen for the swelling solvent.

C. Diffusion under Nonlinear Swelling Protocols. Consider the situation when the swelling comes to a stop after a period t_1. We choose this instant of time so that the volume fraction $\eta = 0.4$ at $t = t_1$. Thus, $t_1 = 160$ ms for $w = 1$, $t_1 = 80$ ms for $w = 2$, and so on. As there is no irreversible process after t_1, $g_w(t)$ does not change at $t > t_1$, and the derivative

$$\frac{\partial}{\partial t} \ln C_w(t_0,t) = -\gamma_0 g_w{}^2(t)$$

becomes constant after the solvent stops growing. The VACFs can be constructed by stitching together the equilibrium solution

$$C_w(t_0,t) = C_w(t_0,t_1) \exp[-\gamma_0 g_w{}^2(t_1)(t - t_1)] \qquad (4.8)$$

if $t > t_1$, and the nonequilibrium solution, eq 4.2, for $t \le t_1$, derived above.

The diffusional behavior of a Brownian particle can be analyzed with the help of the mean-squared displacement

$$\langle r^2(t)\rangle = \langle v^2(0)\rangle \int_0^t \int_0^t C_w(t',t'')\, dt'\, dt'' \qquad (4.9)$$

and the associated exponent

$$\alpha = \frac{d \ln\langle r^2(t)\rangle}{d \ln t}$$

The exponent takes on the value 1 for ordinary diffusion (stochastic trajectories). As is also well-known, α takes on the value 2 if the trajectories are ballistic. Thus, the exponent α is characteristic of the type of dynamics exhibited by a particle.

The observed mean-squared displacements for the Brownian particle in the simulations are shown in Figure 9. The corresponding iLE-based results obtained by numerically integrating eq 4.9 are in near perfect agreement. This is yet another confirmation that the iLE surmises the behavior of the particle model. Equally important, the diffusional behavior is also instructive. The equilibrium limit ($w = 0$) exhibits the usual behavior in which the Brownian particle moves ballistically until its initial collisions and then crosses over to the diffusion regime. The remaining four curves, corresponding to nonzero swelling rates, exhibit more complicated behavior. For larger w, the volume fraction reaches its maximal value (0.4) sooner; the chosen particle interacts with its neighbors sooner, and its average displacement is smaller. But at large t values, the diffusion coefficient, which depends on the final system state only, becomes equal for all four curves and they tend to approach one and the same line with the same slope, namely, the diffusion constant. Figure 9 also shows that α changes nonmonotonically if $w \neq 0$. In fact, this crossover behavior is reminiscent of that seen in glassy dynamics although the solvent

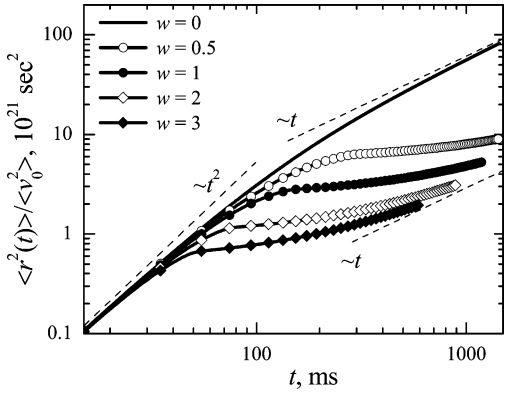

Figure 9. Time dependence of the mean-squared displacement of a Brownian particle in the swelling hard-sphere fluid (theoretical result obtained from eq 4.9). The swelling rate w is shown in nm/ms.

conditions here are always well below the glassy transition. We return to this issue below.

D. Dissipative Dynamics in Swelling Colloidal Suspensions. Colloidal suspensions of noninteracting particles have routinely been modeled using hard-sphere solvents. Because of the simplicity of the latter, it has also been open to a large number of analytic and computer treatments.[18,36,37] Similarly, the swelling-sphere model should be realizable as a colloidal suspension whose average particle diameter changes with time as a consequence of some macroscopic perturbation such as pH or the addition of solutes that bind to (and enlarge) the colloids. The fact that the iLE surmises the VACF of the swelling-sphere model further suggests that the iLE can also surmise the corresponding dynamics of a chosen colloid in a swelling/contracting colloidal suspension. The results above suggest that in the swelling-sphere case, the diffusion of the colloid will be slowed due to the increasing coupling to the swelling solvent. Moreover, the effective diffusion exponent α varies throughout the nonequilibrium solvation.

In refs 38 and 39, colloidal particles in polymer solution exhibit subdiffusive plateaus analogous to those in Figure 9 which are related to yet another process accompanying the particle's motion: the increase of the elastic compliance that leads to a concomitant increase in the shear viscosity at intermediate times. In the glassy regime,[37,39,40] such a plateau has been described as the escape of a particle out of an effective cage where the latter is comprised by the solvent shell for some persistence time. At short times, the cage persists not as a literal physical barrier but rather by slowing down the particle through increased friction as the particle tries to escape through so-called β-relaxation processes.[41,42] Once the particle escapes, it traverses a sufficiently large distance so as to exhibit an increase in the apparent diffusion coefficient. At times much larger than the inverse escape rate, the loss of correlation between consecutive escapes leads to an averaged motion with a smaller diffusion coefficient. A slowing in the diffusion rate has also been seen in ref 43, though they described it using an effective free energy which causes a displacement-dependent caging force that favors localization at certain values of coordinates.

However, the swelling-sphere model system under a swelling profile terminating well below the glass transition volume fraction neither is in the high elasticity regime nor does it exhibit a pronounced caging effect. Nonetheless, it exhibits a plateau in α. This is due to the fact that the particle is being driven by a nonequilibrium (time-dependent) solvent. As in the glassy mechanism, the Brownian particle does feel an effective increase in the friction which slows down its escape from effective cages. The origin of this increasing friction is not the β-relaxation process operative above the freezing temperature. Instead, it is due to the fact that the solvent particles are increasing in size and hence interacting with the Brownian particle sooner than expected. Thus the nonequilibrium solvation gives rise to a glasslike diffusion of the Brownian particle at packing fractions well below the freezing temperature.

As an aside, it should be mentioned that the iLE has also been used to model an alternative nonequilibrium heterogeneous system. In ref 8, the dynamics of a Brownian particle coupled to time-dependent-driven anisotropic heavy particles (mesogens) in a uniform bath (solvent) has been investigated. The rotational motion of the mesogens was assumed to follow the motion of an external driving field in the linear response limit. The periodicity with which the particle's motion is affected by collisions with mesogens results in the oscillatory-type friction and gives rise to successive segments in the time dependence of $\langle R^2 \rangle$.

V. Conclusion

In this paper, a simple explicit particle model, in which the hard-sphere solvent particles swell or contract with time, has been used to represent the role of nonequilibrium solvation in the diffusion of nonideal systems. This model serves two purposes: First, as a demonstration that the irreversible—namely, nonstationary—Langevin equation can indeed surmise the projected dynamics of a complex particle model. Second, to explore the diffusion behavior that emerges from the nonequilibrium solvent using either equivalent representation.

The validity of the iLE has been confirmed using MD simulations of the swelling-sphere model under various nonequilibrium swelling and contracting protocols. The iLE has been seen to describe the dynamics of a Brownian particle in this medium even when the volume fraction changes as quickly as in a rise from 0.002 to 0.5 in less than 100 ms. (Note that even this fast drop has been realized in some of the experiments cited above.) Although the particle model is not explicitly projected onto the iLE, the iLE is fully realized by specifying a coupling function $g(t)$ which fits the results of the numerically generated VACFs over many parameter sets. It has been shown that in the quasi-equilibrium case, at every instant, $g(t)$ can be determined by an instantaneous state of the system. Alternatively, it has also been established that the coupling term $g(t)$, that describes the solvent response in the iLE (a limiting form of the iGLE), naturally stems from the Hamiltonian formalism and appears to be an average coupling amplitude with all the bath modes.

The nonstationarity in the apparent friction of the iLE arises from the macroscopic swelling of the hard-sphere solvent because of two mechanisms: (i) The time to collision between two particles is decreased by the fact that the solute sphere has grown and hence its surface reaches the solute sooner. Moreover, this effect depends on the collision time because the amount of growth is larger at longer collision times. (ii) Near collisions, that would have been avoided under the fixed particle case, can lead to collisions as the collision cross-section increases because of the swelling of the sphere. Both of these mechanisms lead to an increase in the collisions between the solute and the solvent and hence lead to a smaller coherence time (connected to a faster response time) which changes with absolute time.

Typically, the packing fractions explored in this work have been well below the freezing point, and hence, one might not expect that the dynamics would exhibit surprising diffusional behavior. However, the nature of the nonequilibrium coupling between the Brownian particle and the solvent (using the language of the iLE) drives the particle to feel nonequilibrium dissipative forces. The net result is that the diffusion exhibits a subdiffusive plateau at volume fractions characteristic of a liquid. In effect, this suggests that dynamics of particles could be arrested at lower solvent densities if only one subjects them to nonequilibrium driving conditions.

The models described here can, in principle, be realized using colloidal suspensions in which the colloid size is controlled though an external agent. References to experiments and corresponding experimental conditions that have nearly addressed this regime were cited in the Introduction. We hope that the possibility that such nonequilibrium driving forces may give rise to unusual diffusion effects will help motivate a new round of more direct experiments on this issue.

Acknowledgment. This work has been partially supported by the National Science Foundation through Grant No. NSF 02-123320 and 04-43564. R.H. is the Goizueta Foundation Junior Professor.

Appendix: Projection of the Mechanical System

The classical equations of motion, as deduced from Hamiltonian (3.6), can be obtained using the Hamilton−Jacobi equations

$$\dot{x}_i = p_i \tag{A.1}$$

$$\dot{p}_i = -\omega_i^2 x_i + c_i g_i(t) q(t) \tag{A.2}$$

$$\dot{q} = p_q \tag{A.3}$$

$$\dot{p}_q = \sum c_i g_i(t) x_i - \sum \left(\frac{c_i g_i(t)}{\omega_i}\right)^2 q(t) - \frac{\partial}{\partial q(t)} \delta V_2 \tag{A.4}$$

Except for the nonlocal δV_2 term in the last of these equations, the terms are all stationary and the Hamilton−Jacobi equation readily emerges from the variational principle. It turns out that this nonlocal term also emerges from the variational principle, though now one has to use a functional derivative.

Following ref 2, the action corresponding to δV_2, which enters into the Lagrangian in the Euler−Lagrange variational principle, is

$$S_2 = -\int_0^T \delta V_2(q(\cdot),t)\, \mathrm{d}t = -\int_0^T \mathrm{d}t \int_0^t \mathrm{d}t'\, a(t,t') \left[\frac{1}{2} q^2(t') - q(t')q(t)\right]$$

Equating the differential in the action with variations in the function $q(t)$ to zero provides a result

$$\frac{\delta S_2}{\delta q(t)} = \int_0^t \mathrm{d}t'\, a(t,t')q(t') + \int_t^T \mathrm{d}t'\, a(t',t)[q(t') - q(t)] \tag{A.5}$$

for the contribution of δV_2 to the momentum $\dot{q}$. The second term is troubling because it (i) depends on the arbitrary time T and (ii) adds contributions to the force from the future trajectory (seemingly violating causality). The first issue leads to different dynamics depending on the choice of T. But if T is near t, this term vanishes. This suggests that an additional approximation ignoring the second term, and thereby eliminating the transient effects, is warranted. Note, that this is consistent with earlier derivations,[21,44] for the special case of space-dependent friction, in that the transient terms also had to be removed therein but here has the added benefit of restoring causality. That is, while the second issue is not resolved exactly, operationally we ensure causality by ignoring the second term in eq A.5.

Thus, the nonlocal force is approximately given by

$$-\frac{\partial}{\partial q(t)} \delta V_2 = \int_0^t \mathrm{d}t'\, a(t,t')q(t') = \sum g_i(t) \int_0^t \mathrm{d}t' \frac{c_i^2}{\omega_i^2} \cos\omega_i(t-t')\dot{g}_i(t')q(t') \tag{A.6}$$

and this equality is useful in obtaining the result in eq A.13b below.

Returning to the equations of motion, the substitution of eq A.2 into A.1 gives

$$\ddot{x}_i + \omega_i^2 x_i = c_i g_i(t) q(t) \tag{A.7}$$

Performing the Laplace transform ($\tilde{f}(s) = \int_0^\infty \exp(-st) f(t)\, \mathrm{d}t$) of this equation, yields

$$(s^2 + \omega_i^2)\tilde{x}_i(s) - s x_i(0) - \dot{x}_i(0) = c_i\, \tilde{G}_i(s) \tag{A.8}$$

where $\tilde{G}_i(s) \equiv \int_0^\infty \exp(-st) g_i(t) q(t)\, \mathrm{d}t$. Solving the algebraic equations in s-space leads to

$$\tilde{x}_i(s) = \frac{s}{s^2 + \omega_i^2} x_i(0) + \frac{1}{s^2 + \omega_i^2} p_i(0) + \frac{c_i}{s^2 + \omega_i^2} \tilde{G}_i(s) \tag{A.9}$$

(here, of course, $p_i(0) = \dot{x}_i(0)$). Since the last term in eq A.9 can be rearranged as

$$\frac{c_i}{\omega_i^2}\left[\tilde{G}_i(s) - \frac{s}{s^2 + \omega_i^2}(s\tilde{G}_i(s) - g_i(0)q(0))\right] - \frac{c_i}{\omega_i^2} \frac{s}{s^2 + \omega_i^2} q(0) \tag{A.10}$$

the inverse Laplace transform of eq A.9 gives

$$x_i = x_i(0)\cos(\omega_i t) + p_i(0)\frac{\sin(\omega_i t)}{\omega_i} + \frac{c_i}{\omega_i^2} g_i(t) q(t) \tag{A.11}$$

$$-\frac{c_i}{\omega_i^2}\int_0^t \mathrm{d}t' \cos(\omega_i(t-t'))\frac{\mathrm{d}}{\mathrm{d}t'}(g_i(t')q(t')) - \frac{c_i}{\omega_i^2} q(0)\cos(\omega_i t)$$

To obtain this result, the initial condition in eq 3.9 is used together with the rule $\tilde{\dot{f}}(s) = s\tilde{f}(s) - f(0)$. Using eq A.11 in eq A.4, we can write

$$\ddot{q} = \sum \left(c_i g_i(t) x_i(0) \cos\omega_i t + \frac{c_i}{\omega_i} g_i(t) p_i(0) \sin\omega_i t\right) \tag{A.12}$$

$$-\sum \frac{c_i^2}{\omega_i^2} g_i(t) \int_0^t \cos(\omega_i(t-t'))\frac{\mathrm{d}}{\mathrm{d}t'}(g_i(t')q(t'))\, \mathrm{d}t'$$

$$-\sum \frac{c_i^2}{\omega_i^2} g_i(t) q(0) \cos\omega_i t - \frac{\partial}{\partial q(t)} \delta V_2$$

Thus, the iGLE originating from Hamiltonian (3.6), reads

$$\ddot{q} = -\int_0^t \gamma(t,t')\dot{q}(t')\, \mathrm{d}t' + \xi(t) - \sum \frac{c_i^2}{\omega_i^2} g_i(t) \int_0^t \cos\omega_i(t-t')\dot{g}_i(t')q(t')\, \mathrm{d}t' - \frac{\partial}{\partial q(t)} \delta V_2 \tag{A.13a}$$

$$= -\int_0^t \gamma(t,t')\dot{q}(t')\, \mathrm{d}t' + \xi(t) \tag{A.13b}$$

where $\gamma(t,t')$ and $\xi(t)$ are defined in eqs 3.11 and 3.12, and the second equality follows from eq A.6.

If the initial distribution is Boltzmann as per

$$P \sim \exp\left[-\frac{\beta}{2}\sum\left(p_i^2(0) + \left(\omega_i x_i(0) - \frac{c_i}{\omega_i}q(0)\right)^2\right)\right] \quad \text{(A.14)}$$

with $1/\beta = k_B T$, then

$$\langle p_i(0)p_j(0)\rangle = \beta^{-1}\delta_{ij} \quad \text{(A.15)}$$

$$\left\langle\left(\omega_i x_i(0) - \frac{c_i}{\omega_i}q(0)\right)\left(\omega_j x_j(0) - \frac{c_j}{\omega_j}q(0)\right)\right\rangle = \beta^{-1}\delta_{ij} \quad \text{(A.16)}$$

$$\left\langle p_i(0)\left(\omega_j x_j(0) - \frac{c_j}{\omega_j}q(0)\right)\right\rangle = 0 \quad \text{(A.17)}$$

and one can write

$$\langle \xi(t)\xi(t')\rangle = \frac{1}{\beta}\sum\left(\frac{c_i}{\omega_i}\right)^2 g_i(t)g_i(t')\cos\omega_i(t-t') \quad \text{(A.18)}$$

This means that the FDR (3.13) is satisfied.

References and Notes

(1) Hernandez, R. *J. Chem. Phys.* **1999**, *111*, 7701.
(2) Vogt, M.; Hernandez, R. *J. Chem. Phys.* **2005**, *123*, 144109.
(3) Hernandez, R.; Somer, F. L. *J. Phys. Chem. B* **1999**, *103*, 1064.
(4) Hernandez, R.; Somer, F. L. *J. Phys. Chem. B* **1999**, *103*, 1070.
(5) Somer, F. L.; Hernandez, R. *J. Phys. Chem. A* **1999**, *103*, 11004.
(6) Somer, F. L.; Hernandez, R. *J. Phys. Chem. B* **2000**, *104*, 3456.
(7) Drozdov, A. N.; Tucker, S. C. *J. Phys. Chem. B* **2001**, *105*, 6675.
(8) Hershkovitz, E.; Hernandez, R. *J. Chem. Phys.* **2005**, *122*, 014509.
(9) Jones, C. D.; Lyon, L. A. *Macromolecules* **2000**, *33*, 8301.
(10) Fernandez-Nieves, A.; Fernandez-Barbero, A.; Vincent, B.; Nieves, de las F. J. *Macromolecules* **2000**, *33*, 2114.
(11) Fernandez-Nieves, A.; Fernandez-Barbero, A.; Vincent, B.; Nieves, de las F. J. *Prog. Colloid Polym. Sci.* **2000**, *115*, 134.
(12) Garcia-Salinas, M. J.; Romero-Cano, M. S.; Nieves, de las F. J. *Prog. Colloid Polym. Sci.* **2001**, *118*, 180.
(13) Fernandez-Nieves, A.; Fernandez-Barbero, A.; Nieves, de las F. J. *J. Chem. Phys.* **2001**, *115*, 7644.
(14) Wang, J.; Gan, D.; Lyon, L. A.; El-Sayed, M. A. *J. Am. Chem. Soc.* **2001**, *123*, 11284.
(15) Fernandez-Nieves, A.; Fernandez-Barbero, A.; Vincent, B.; Nieves, de las F. J. *J. Chem. Phys.* **2003**, *119*, 10383.
(16) Pelton, R. *Adv. Colloids Interface Sci.* **2000**, *85*, 1.
(17) Fernandez-Nieves, A.; Fernandez-Barbero, A.; Grillo, I.; Lopez-Cabarcos, E. *Phys. Rev. E* **2002**, *66*, 051803.
(18) Allen, M. P.; Tildesley, D. J. *Computer Simulations of Liquids*; Oxford: New York, 1987.
(19) Lindenberg, K.; Seshadri, V. *Physica A* **1981**, *109*, 483.
(20) Carmeli, B.; Nitzan, A. *Phys. Rev. Lett.* **1982**, *49*, 423.
(21) Carmeli, B.; Nitzan, A. *Chem. Phys. Lett.* **1983**, *102*, 517.
(22) Lindenberg, K.; Shuler, K. E.; Seshadri, V.; West, B. J. In *Probabilistic Analysis and Related Topics*; Bharucha-Reid, A. T., Ed.; Academic Press: New York, 1983; Vol. 3, pp 81−125.
(23) Lindenberg, K.; Cortés, E. *Physica A* **1984**, *126*, 489.
(24) Pollak, E.; Berezhkovskii, A. M. *J. Chem. Phys.* **1993**, *99*, 1344.
(25) Bao, J. D.; Abe, Y.; Zhuo, Y. Z. *Phys. Rev. E* **1998**, *58*, 2931.
(26) Bao, J. D.; Li, R. W.; Wu, W. *J. Comput. Phys.* **2004**, *197*, 241.
(27) Kneller, G. R.; Sutmann, G. *J. Chem. Phys.* **2004**, *120*, 1667.
(28) Zwanzig, R. *J. Stat. Phys.* **1973**, *9*, 215.
(29) Caldeira, A. O.; Leggett, A. J. *Physica A* **1983**, *121*, 587.
(30) Hänggi, P.; Talkner, P.; Borkovec, M. *Rev. Mod. Phys.* **1990**, *62*, 251, and references therein.
(31) Hoover, W. G.; Ree, F. H. *J. Chem. Phys.* **1968**, *49*, 3609.
(32) Pusey, P. N.; Megen, van W. *Nature* **1986**, *320*, 340.
(33) Chapman, S.; Cowling, T. G. *The Mathematical Theory of Nonuniform Gases*; Cambridge University Press: New York, 1995.
(34) Burshtein, A. I.; Krongauz, M. V. *J. Chem. Phys.* **1995**, *102*, 2881.
(35) Burshtein, A. I. *J. Chem. Phys.* **1995**, *103*, 9515.
(36) Hansen, J. P.; McDonald, I. R. *Theory of Simple Liquids*; Academic Press: San Diego, CA, 1986.
(37) Götze, W. *Liquids, Freezing and the Glass Transition*; North-Holland: Amsterdam, The Netherlands, 1991.
(38) Zanten, van J. H.; Amin, S.; Abdala, A. A. *Macromolecules* **2004**, *37*, 3874.
(39) Wong, I. Y.; Gardel, M. L.; Reichman, D. R.; Weeks, E. R.; Valentine, M. T.; Bausch, A. R.; Weitz, D. A. *Phys. Rev. Lett.* **2004**, *92*, 178101.
(40) Götze, W. *J. Phys.: Condens. Matter* **1999**, *11*, A1.
(41) Fuchs, M.; Götze, W.; Hildebrand, S.; Latz, A. *J. Phys.: Condens. Matter* **1992**, *4*, 7709.
(42) Götze, W.; Sjögren, L. *Rep. Prog. Phys.* **1992**, *55*, 241.
(43) Chen, Y.-L.; Kobelev, V.; Schweizer, K. S. *Phys. Rev. E* **2005**, *71*, 041405.
(44) Cortés, E.; West, B. J.; Lindenberg, K. *J. Chem. Phys.* **1985**, *82*, 2708.